Hypersonic Research Project Memo 69, Aug. 1963, California Institute of Technology, Pasadena, Calif.

[19] Kelly, H. R., "An Analytical Method for Predicting the Magnus Force and Moments on Spinning Projectiles," TM-1634, 1954, U.S. Naval Ordnance Test Station, China Lake, Calif.

[20] Jones, D. L., "Tables of Inviscid Supersonic Flow about Circular Cones at Incidence $\gamma = 1.4$," AGARD 137, 1969.

[21] Mayne, A. W., "Analysis of Laminar Boundary Layers on Right Circular Cones at Angle of Attack, Including Streamline-Swallowing Effects," AEDC-TR-72-134, Oct. 1972, Arnold Engineering Development Center, Tullahoma, Tenn.

[22] Curry, W. H., Reed, J. F., and Ragsdale, W. C., "Magnus Data on the Standard 10° Cone Calibration Model," SC-DC 71-3821, 1971, Sandia Laboratories, Albuquerque, N. Mex.

[23] Ward, G. N., "Supersonic Flow Past Slender Pointed Bodies," *Quarterly Journal of Mechanics and Applied Mathematics*, Vol. 2, No. 1, March 1949, p. 75.

[24] Moore, F., "Displacement Effect of a Three-Dimensional Boundary Layer," TN 2722, 1952, NACA.

[25] Curry, W. H., Platou, A. S., and Reynold, W. C., "Magnus Characteristics of a 10° Cone at Supersonic Mach Numbers," Research Rept., Sandia Laboratories, Albuquerque, N. Mex. (to be published).

[26] Lighthill, M. J., *Laminar Boundary Layers*, edited by L. Rosenhead, Oxford Press, New York, 1963, pp. 1–113.

JULY 1974 AIAA JOURNAL VOL. 12, NO. 7

Prediction of the Critical Diameter of Composite Propellants

P. K. SALZMAN* AND T. C. DUNCAN†
General Dynamics, Pomona, Calif.

A theoretical model which predicts the critical diameter of composite propellants is presented. A previously published detonation model is corrected and refined by use of a new model which considers both single grain size AP and dual grain size AP configurations, for both porous and nonporous propellants. Both ignition due to shock heating of the AP and compression heating of gas-filled voids are considered. By comparison of results with experimental data for an AP-PBAN-Al propellant, an "intrinsic" porosity of 0.22% was established for nominally "nonporous" propellants. Using this value, a critical diameter of 3.0 ft is predicted for a nonaluminized AP propellant.

Nomenclature

a = length of a face centered cube (fcc)
a_o = nearest neighbor distance in a fcc
B = oxidizer burning rate
$\bar{B}$ = average burning rate
d = diameter
d_c = critical diameter
δ = diffusion/burning distance
δ_d = diffusion distance
D = detonation velocity
D_i = ideal detonation velocity
$\mathcal{D}$ = diffusion coefficient
ξ = reaction zone thickness
γ_g = Gruneisen's constant
n_p = total number of voids
N = number of "effective" voids (ignition sites)
P = propellant porosity
Q = heat of reaction
ρ = density
r_a = void radius
R_G = oxidizer grain radius
R_e = total burning distance
t = time
t_i = ignition time
t_o = oxidizer burning time
t_b = binder burning time
t_{ob} = oxidizer/binder burning time, nonconsecutive process
T = temperature
X = mass fraction

Subscripts
a = ambient conditions
Al = aluminum
B = binder
G = oxidizer (AP)
L = large grain
n = nonporous
S = small grain

Introduction

THE most important parameter in evaluating the detonability of a given substance is the critical diameter d_c. For composite propellants a theoretical method was developed[1] for predicting d_c based on an analysis of the events occurring in the reaction zone. It was shown that the d_c for nonporous propellant was quite high (~50 ft) but that it decreased rapidly with porosity P ($d_c \approx 1$ ft at $P \approx 5\%$). However, a subsequent experimental program[2] showed that d_c for (nonporous) composite propellants was actually much lower than predicted (~5 ft). The general objectives of the current study were to: 1) reconcile the differences in theory and experiment and develop an improved detonation model; and 2) apply the model to an AP-PVC/DOA propellant‡ to determine its d_c.

Detonation Model

The detonation model employed in this study is essentially that used in Ref. 1. The nozzle theory of Jones[3] is used to

Received November 27, 1972; presented as Paper 72-1117 at the AIAA/SAE 8th Joint Propulsion Specialist Conference, New Orleans, La., November 29–December 1, 1972; revision received October 29, 1973.

Index categories: Fuels and Propellants, Properties of; Shock Waves and Detonations; Combustion Stability, Ignition, and Detonation.

* Section Head, Aerothermodynamics Section. Member AIAA.
† Design Specialist.

‡ AP = Ammonium Perchlorate; PVC = Polyvinyl Chloride; and DOA = Di-Octyl Adipate.

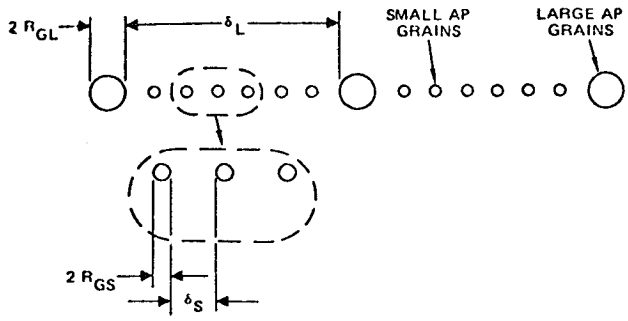

Fig. 1 Nonporous dual grain model.

describe nonideal detonation in terms of the reaction zone thickness, the approximation of Eyring et al.[4] is used to relate this thickness to reaction time, and the model of Andersen and Chaiken[5] is used to evaluate this time in terms of processes occurring in the reaction zone. The method of critical diameter determination is similar to that given by Evans.[6]

Jones' nozzle theory for uncased cylindrical charges can be written[3]

$$(D/D_i)^2 = 1-3.2(\xi/d)^2 \tag{1}$$

where D is the (steady) detonation velocity at diameter d, D_i is the ideal detonation velocity, and ξ is the reaction-zone thickness. The reaction time t is related to ξ by[4]

$$t \cong 4\xi/3D \tag{2}$$

and simultaneous solution of Eqs. (1) and (2) results in

$$t = \left(\frac{5}{9}\right)^{1/2}\left(\frac{d}{D}\right)\left[1-\left(\frac{D}{D_i}\right)^2\right]^{1/2} \tag{3}$$

In this relation t functionally depends on D; d and D_i are system parameters.

The ideal detonation velocity D_i is dependent only on the specific energy of the material and is given by[7] $D_i^2 = 8.32\times 10^{-3}\gamma_g\ (\gamma_g+2)Q$, where Q is the heat of reaction (cal/100 gm) and γ_g is Gruneisen's constant.

Andersen and Chaiken's approach[5] and that taken by Salzman et al.[1] assumes that the events occurring in the reaction zone are, consecutively; 1) shock ignition of the oxidizer (ammonium perchlorate, AP), 2) burning of the oxidizer grain, and 3) burning of the binder. The total reaction time is given by

$$t = t_i+t_o+t_b \tag{4}$$

where t_i, t_o, and t_b refer to the time required for each individual event. When each of these times is related to D and/or any other system parameters, d_c is found by the unique intersection of Eqs. (3) and (4).[1,6]

In this study, we also consider the possibility that binder might burn while the oxidizer burns and thus that the processes are not consecutive. In this case Eq. (4) becomes

$$t = t_i+t_{ob} \tag{5}$$

where the latter term is either the combined burning time of oxidizer and binder or, in some cases, simply the larger of the two.

Expressions for these reaction times are presented for nonporous and porous propellants, single grain size and dual grain size, in the following paragraphs.

Nonporous Propellant

For nonporous propellant, the assumption of consecutive events [and thus the use of Eq. (4)] was justified by showing that the shocked AP was hotter than the binder.[1] Binder burning would not begin until essentially all the AP had been consumed. Therefore for a propellant with AP particles (of any single size) the assumption of consecutive process is supported if the AP is hotter than the binder under shock loading.

On the other hand, for a propellant with a distribution of AP grain sizes, the argument presented[1] would not obtain. Smaller AP particles would equilibrate with the binder rapidly while only the larger ones would remain at a high temperature and ignite first. The subsequent burning would involve both binder *and* the smaller oxidizer particles. Consecutive processes would not be a valid assumption. Since for real propellants, various AP grain sizes are expected, the use of Eq. (4) in this instance is clearly questionable. However to demonstrate the validity of the calculation methods and refine the prior results,[1] a model for the single grain case was developed. To determine if the known results in Ref. 2 could be predicted and the d_c of AP-PVC/DOA estimated, a (more realistic) dual grain model was also developed.

Single Grain Model

For the single grain model Eq. (4) obtains, since consecutive processes are considered valid.

Shock Ignition Time—t_i

Since ignition occurs by shock heating, t_i is given by Eqs. (5–8, 11) of Ref. 1 as a function of temperature. As the shock temperature of the AP particles is usually different from that of the binder, it is necessary to consider the transient behavior of both the large and small AP grains to determine the appropriate temperature to use. Calculations indicate that large grains ($R_G \approx 100\mu$) tend to remain at their shock temperatures during ignition, while small grains ($R_G \approx 10\mu$) generally will have the equilibrated temperature of the AP and binder. Medium sized grains will have ignition temperatures that depend on the local transient heat conduction.

Oxidizer Burning Time—t_o

For pure AP, the grain burning time is given by $t_o = R_G/B$, where B is the burning rate given by Eqs. (23) and (24) of Ref. 1.

Binder Burning Time—t_b

The binder must first be vaporized and mixed with the oxidizer gases before combustion occurs, resulting in a diffusion controlled process (the reaction is assumed to be fast). Assuming that there is laminar mixing and that the average binder thickness is small, the burning time is given by[6] $t_b = \delta_d^2/2\mathscr{D}$, where δ_d is the diffusion distance (equal to one-half the binder thickness between grains). The diffusion coefficient $\mathscr{D}$ is given by[1]

$$\mathscr{D} = \mathscr{D}_a\left(\frac{\rho_a}{\rho}\right)\left(\frac{T}{T_a}\right)^{3/4} \tag{6}$$

where the subscript a refers to ambient conditions. Values[1] of 0.15 cm^2/sec, 0.002 g/cc, and 300°K were used for $\mathscr{D}_a$, ρ_a, and T_a, respectively, in this analysis.

The diffusion distance δ_d is determined by assuming; 1) that all the AP grains are of equal size, spherical, and packed (on the average) in a face-centered cubic (fcc) arrangement; and 2) that the binder is generally composed of aluminum and some organic binder (which might be a mixture of several substances). The length of a side of the unit cube is given by

$$a = R_G\left[\left(\frac{16\pi}{3}\right)\left(1+\frac{X_B}{X_G}\frac{\rho_G}{\rho_B}+\frac{X_{Al}}{X_G}\frac{\rho_G}{\rho_{Al}}\right)\right]^{1/3} \tag{7}$$

where X_B, X_G, and X_{Al} are the mass fractions of the binder, AP, and aluminum, respectively, and the ρ's are the corresponding densities. The diffusion distance, the half-distance between two AP particles in the fcc arrangement, is then given by

$$\delta_d = \frac{1}{2}\left(\frac{a}{(2)^{1/2}}-2R_G\right) = \frac{R_G}{2}\left\{\frac{(2)^{1/2}}{2}\left[\left(\frac{16\pi}{3}\right)\times\left(1+\frac{X_B}{X_G}\frac{\rho_G}{\rho_B}+\frac{X_{Al}}{X_G}\frac{\rho_G}{\rho_{Al}}\right)\right]^{1/3}-2\right\} \tag{8}$$

Dual Grain Model

As an approximation to a real propellant two AP grain sizes (only) are assumed to exist in the binder. Generally, composite propellants use a blend of unground (large) and ground (small) AP particles. Although each has a size distribution about their respective means, the use of two sizes is fundamentally realistic. The large grains have $R_G \gtrsim 100\mu$ and the small ones $R_G \lesssim 10\mu$ (i.e., there are no "medium" sized grains). In this instance, the former remain at the shock temperature during ignition whereas the latter equilibrate with the binder.

Since the large grains (essentially) remain at the shock temperature, effectively the whole particle woud be consumed in the thermal explosion; there would be no subsequent (large) grain burning. The binder and remaining small AP grains would then ignite and burn concurrently. In this case Eq. (5) obtains.

For the dual grain system, the possibility that the binder does not burn sufficiently fast to contribute to the detonation process can be considered. Physically, the large and small AP grains would be so configured that each of them touches at least one other and/or the binder thickness between grains is very thin. In either case the oxidizer burning in one grain will lead to ignition of adjacent grains with "negligible" time delay. In this case Eq. (4) would apply with $t_b \equiv 0$. Of course, if the binder does not burn, account must be taken of this fact by reducing Q in the equation for D_i by the amount of heat evolved in binder burning.

The shock ignition time, t_i is again given as in Ref. 1 and as aforementioned; for large particle radii $\gtrsim 100\mu$, the oxidizer burning time, t_o, is zero.

The binder/small oxidizer burning model is shown in Fig. 1. Since ignition always occurs at a large particle, the propagation of the reaction through the small particle/binder mixture may be visualized as grain burning followed by binder burning repeated one-half as many times as small particles between the large ones. In this case, the small grain burning distance is $2R_{GS}$ and the diffusion length, $\delta_d = \delta_S$. Thus t_{ob} will be the average time to burn through one-half the distance between large grains. The total burning distance is then $\delta_L/2$, the incremental burning distance is $\delta_S + 2R_{GS}$, and the incremental burning time is $\delta_S^2/2\mathscr{D} + 2R_{GS}/B$. The radii, R_{GS} and R_{GL}, and distances, δ_S and δ_L, are defined in Fig. 1, and $\mathscr{D}$ and B are given by Eq. (6) and Ref. 1, respectively.

The total burning time is given by§

$$t_{ob} = \frac{\delta_L}{2(2R_{GS}+\delta_S)}\left[\frac{1}{2}\frac{\delta_S^2}{\mathscr{D}} + \frac{2R_{GS}}{B}\right] \tag{9}$$

The distances δ_L and δ_S may be defined as follows. It is assumed that all the AP grains are spherical and of only the two sizes under consideration. The large particles are assumed to be distributed in an fcc arrangement independent of the small ones which are included (for this purpose) as binder. The derivation in Eqs. (7–8) then applies except that an extra term is required (to account for the volume of the small AP grains) and the distance of interest is δ_L (not one-half of δ_L). This results in

$$\delta_L = R_{GL}\left\{\frac{(2)^{1/2}}{2}\left[\left(\frac{16\pi}{3}\right)\left(1 + \frac{X_B}{X_{GL}}\frac{\rho_G}{\rho_B} + \frac{X_{Al}}{X_{GL}}\frac{\rho_G}{\rho_{Al}} + \frac{X_{GS}}{X_{GL}}\right)\right]^{1/3} - 2\right\} \tag{10}$$

where X_{GL} and X_{GS} are the mass fractions of the large and small AP grains, respectively.

The small grains are also assumed to be distributed in an fcc lattice, the presence of the large grains being ignored. Again, the derivation in Eqs. (7) and (8) applies, except that the mass fractions of interest change and the distance of interest is δ_S (not $\delta_S/2$).

The result is

$$\delta_S = R_{GS}\left\{\frac{(2)^{1/2}}{2}\left[\left(\frac{16\pi}{3}\right)\left(1 + \frac{X_B}{X_{GS}}\frac{\rho_G}{\rho_B} + \frac{X_{Al}}{X_{GS}}\frac{\rho_G}{\rho_{Al}}\right)\right]^{1/3} - 2\right\} \tag{11}$$

§ If binder burning does not occur, $\delta_S \simeq 0$ and Eq. (9) becomes $t_{ob} = t_o = \delta_L/2B$.

Porous Propellant

For porous propellant, we assume that a distribution of voids serves as "hot-spot" ignition sites for the AP grains. It is also assumed that the shock velocities required to "activate" a hot spot are well below those required for fast thermal decomposition of the grains as in the nonporous case. Because the distance between ignition sites is expected to be large (greater than the distance between large grains), subsequent burning between sites will include both AP (single and/or dual sizes) and binder, and Eq. (5) is applicable.

Single Grain Model

The single grain porous model is essentially that developed in Ref. 1.

Shock Ignition Time—t_i

Shock compression of voids in the oxidizer-binder matrix is expected to lead to temperatures[4] sufficiently high to cause ignition of adjacent AP grains in very short times, resulting in $t_i \cong 0$.

Oxidizer/Binder Burning Time—t_{ob}

In this case, the distance between ignition sites may be visualized as in Fig. 2, in which the ignition sites (voids) are again in a face-centered cubic arrangement. The effective burning distance is one-half the average distance between the edge of the sites, R_e, and the oxidizer/binder burning time may be defined by $t_{ob} = R_e/\bar{B}$, where $\bar{B}$ is the average burning rate of the alternate binder/oxidizer/binder, etc., reactions.

The number of effective voids (ignition sites) is a function of the total number of voids n_p, void size distribution, propellant porosity P, and shock velocity D, which controls the void temperature. The equation defining this number of effective voids N is presented in Ref. 1 as $N = n_p \exp[-k_1 n_p/PD^2]$ in which k_1 is a constant. It is assumed that each AP grain has a void associated with it. Thus, using Eq. (7) for an fcc arrangement

$$n_p = \frac{3}{4\pi R_G^3\left[1 + \frac{X_B}{X_G}\frac{\rho_G}{\rho_B} + \frac{X_{Al}}{X_G}\frac{\rho_G}{\rho_{Al}}\right]} \tag{12}$$

It is assumed that the N effective voids are also distributed in an fcc arrangement as shown in Fig. 2. In this case $R_e = a_o/2 - r_a$, where a_o is the nearest neighbor distance in the fcc arrangement and r_a is the void radius. Noting that $a_o = a/(2)^{1/2}$, $N = 4/a^3$, $v_a = P/n_p$, and $(4/3)\pi r_a^3 = v_a$ (assuming spherical voids) and substituting for N gives

$$R_e = 0.561 n_p^{-1/3}\left[e^{k_1 n_p/3PD^2} - 1.105P^{1/3}\right] \tag{13}$$

which, along with Eq. (12) defines R_e for any value of P. Utilizing data for porous AP,[1] develops a value for k_1 of 0.7 cm^3m^2/sec^2.

The average burning rate $\bar{B}$ can be determined from Fig. 2 in which the incremental burning distance is $\delta + 2R_G$, and the incremental burning time is $\delta^2/2\mathscr{D} + 2R_G/B$. The average burning rate is then given by

$$\bar{B} = \frac{\delta + 2R_G}{\frac{1}{2}(\delta^2/\mathscr{D}) + (2R_G/B)} \tag{14}$$

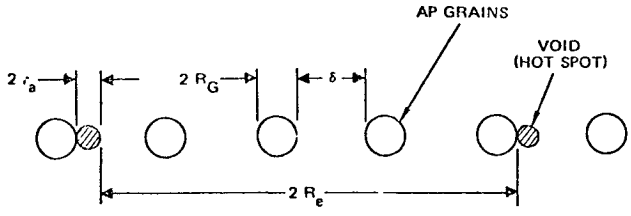

Fig. 2 Porous propellant single grain model.

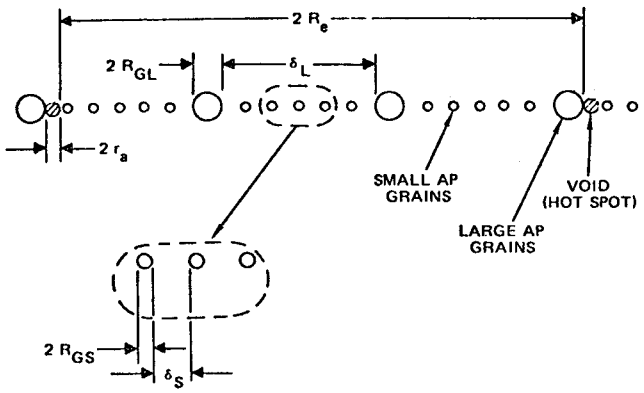

Fig. 3 Porous dual grain model.

The distance between grains δ is again given by Eqs. (7) and (8) except that the distance of interest (i.e., δ_d) is δ (not $\delta/2$). The result is

$$\delta = R_G\left\{\frac{(2)^{1/2}}{2}\left[\left(\frac{16\pi}{3}\right)\left(1+\frac{X_B}{X_G}\frac{\rho_G}{\rho_B}+\frac{X_{Al}}{X_G}\frac{\rho_G}{\rho_{Al}}\right)\right]^{1/3}-2\right\} \quad (15)$$

Dual Grain Model

This more realistic case combines the dual grain nonporous model with the single grain porous model. It is assumed that the addition of small AP grains does not add any voids to the system. Therefore ignition will take place at hot spots adjacent to the large oxidizer grains and subsequent burning will involve these large grains as well as the binder and small oxidizer grains. Equation (5) is clearly applicable in this case.

As in the prior case the voids are assumed to ignite the (large) AP grains very rapidly and $t_i \cong 0$. Considering the large oxidizer/binder/small oxidizer burning time t_{ob}, the burning distances may be visualized as in Fig. 3. Since the voids are associated with the large particles only, Eqs. (12–14) obtain except that Eq. (12) is replaced by

$$n_p = \frac{3}{4\pi R_{GL}^3\left(1+\frac{X_B}{X_{GL}}\frac{\rho_G}{\rho_B}+\frac{X_{Al}}{X_{GL}}\frac{\rho_G}{\rho_{Al}}+\frac{X_{GS}}{X_{GL}}\right)} \quad (16)$$

The average burning rate $\bar{B}$ in this case can be determined from Fig. 3 from which the burning distances and times can be evaluated, as was done for the single grain model except that now the burning of the small grains must also be included. This results in a burning rate given by

$$\bar{B} = \frac{\delta_L + 2R_{GL}}{\left(\frac{\delta_L}{\delta_S+2R_{GS}}\right)\left(\frac{1}{2}\frac{\delta_S^2}{\mathscr{D}}+\frac{2R_{GS}}{B}\right)+\frac{2R_{GL}}{B}} \quad (17)$$

The distances of interest δ_L and δ_S are given by Eqs. (10) and (11). If binder burning does not occur $\delta_S \approx 0$ and $\bar{B} = B$.

Intrinsic Porosity

The theory developed for porous propellant assumes a distribution of voids that act as "hot-spot" igniters of AP grains. The average void volume is directly related to both the number of voids and the propellant porosity. It is tacitly assumed that, as $\rho_o \to \rho_{on}$, $P \to 0$, $v_a \to 0$, and $N \to 0$ (independent of n_p). That is, as the propellant density approaches the nonporous density, the porosity, average pore volume, and number of effective sites approach zero regardless of the total number of voids. This is clearly the nonporous case and the appropriate theory would apply.

However, there is some doubt that this ever occurs in real propellants. Considering current manufacturing techniques, the complete elimination of all pore spaces is considered unlikely. It is expected that a small residual porosity exists and that $\rho_o < \rho_{on}$. Unfortunately, a quantitative estimate of this residual is not available.

In addition to voids, it is expected that under shock loading, other "hot-spot" sites suitable for igniting AP will also exist in the propellant. These might include crystal flaws or defects,[1] load-bearing contact points,[4] shock interactions,[2] blanched regions, phenoblasts,[8] etc. As the total porosity is decreased, these "inherent" sites could become significant and play (perhaps) a major role when the minimum (residual) porosity is reached. Since it is expected that the number of effective sites will increase with D (as do voids) they are considered to be "equivalent" voids, and the functionality with D is assumed to be the same as for voids.

The sum of the "actual" residual voids and the "equivalent" voids (i.e., the "inherent" sites) is defined as the intrinsic porosity. This is expected to lead to critical diameters less than those computed for the "nonporous" case which is now considered academic (i.e., *all* propellants are porous). The intrinsic porosity is expected to be a "real" property of all propellants.

Although a quantitative evaluation of intrinsic porosity is not possible, reasonable upper and lower bounds may be estimated. A value greater than 0.01 (at least for residual porosity) would probably be detectable in density and/or photomicrographic measurements and since it is not, would serve as an upper bound. A value less than 0.001 would lead to a negligibly

Table 1 Propellant properties of interest

Propellant	Constituent	X	ρ_o g/cc	R_G μ	$-\Delta H_f$ Kcal/100 g	C_v cal/g-°K	$(\partial P/\partial T)_{v_o}$ dynes/cm²-°K
AP-PU[1]	AP	0.75	1.95	50	70.73[9]	[a]	3.32×10^7
ρ_o = 1.60 g/cc	PU	0.25	1.07	...	82.8	[b]	1.45×10^5
ANB-3226	AP	0.69	1.95	...			
ρ_o = 1.73 g/cc	Large	0.483	1.95	86			
	Small	0.207	1.95	3			
	PBAN	0.16	1.02	...			
	Al	0.15	2.70	...			
AP-PVC/DOA	AP	0.81	1.95	...	70.73	[a]	3.32×10^7
ρ_o = 1.705 g/cc	Large	0.232	1.95	97.5	70.73	[a]	3.32×10^7
	Small	0.578	1.95	10	70.73	[a]	3.32×10^7
	PVC/DOA	0.19	1.10	...	...	0.47	2.18×10^6
	PVC	0.083	1.50	...	330.0	...	...
	DOA	0.107	0.925	...	84.9	...	...

[a] $C_v = 0.264 + 1.74\times10^{-4}\,(T-300°K)$.
[b] $C_v = 0.39 + 4.3\times10^{-4}\,(T-300°K)$.

small fraction of effective voids even at relatively high shock velocities, and represents a lower bound. The consistency of these estimates with the critical diameter determinations for the various propellants is considered in the following discussion.

Results and Discussion

The theory presented in the preceding section was utilized to predict the critical diameters of three composite propellants; AP-PU, ANB-3226, and AP-PVC/DOA.¶ The compositions and other properties of these propellants are presented in Table 1. The AP-PU propellant was analyzed in order to verify the mathematical techniques of the theory and refine the results of Ref. 1. The validity of the theory was investigated by analyzing ANB-3226 as the critical diameter and detonation velocity of this propellant are known.[2] Based on the information gained in these two analyses, the critical diameter and detonation velocity of the AP-PVC/DOA propellant were predicted.

Critical Diameter of AP-PU Propellant

Considering first the nonporous case, the Hugoniot temperature was determined and the ignition time t_i was then obtained as a function of D/D_i. For grains of the given size, $R_G = 50\mu$, the center will not have cooled significantly and shock ignition will begin at the AP Hugoniot temperature. After the center ignites, the grain will burn outward, giving an oxidizer burning distance of $R_G = 50\mu$.

The diffusion distance, δ_d is given by Eq. (8). A density of 1.333 ρ_o and an average Chapman-Jouget temperature of 2390°K were used in Eq. (6). (This temperature is essentially constant over the detonation velocity range of interest,[1] ~6300 m/sec.)

The resulting critical diameter, presented in Table 2, was found to be 12.1 ft, which is much less than the 55.5 ft predicted in Ref. 1. This is primarily due to a more accurate digital computer solution for the Hugoniot shock temperature of the AP which resulted in higher temperatures and thus in much shorter ignition times (see Table 2). The binder burning time was also reduced because of an error in the equation originally given.[1] In light of the d_c found for the SOPHY[2] propellant (~6 ft), this latest value seems quite reasonable.

Next, the critical diameter for the single grain porous case was computed, using the appropriate previously discussed equations. The diffusion rates and oxidizer burning rates, $\mathscr{D}$ and B, were uniformly evaluated at a detonation velocity of 3200 m/sec (the Chapman-Jouget temperature of 2025°K, Ref. 1, was used), as this is the approximate expected critical detonation velocity.[2] This gives an oxidizer burn rate B of 200 cm/sec and a $\mathscr{D}$ of 5.90×10^{-4} cm^2/sec. Detonation velocities other than 3200 m/sec will have very little effect on $\mathscr{D}$. A sensitivity check on B indicated that for a ± 800 m/sec variation in detonation velocity, the critical diameter predicted for ANB-3226 and AP-PVC/DOA (using the $B = 200$) is in error by only ~12%. Since the values of D_c predicted in both cases are generally close to 3200 m/sec (at the intrinsic porosity discussed later) the error in using a constant B is considered small.

Table 2 Nonporous solution results

		AP-PU	ANB-3226	AP-PVC/DOA
D_i	m/sec	6550	6700	5820
t_{ic}	msec	0.044	0.030	2.8
t_{oc}	msec	0.009	...	...
t_{obc}	msec	...	0.055	$\ll t_{ic}$
t_c	msec	0.126	0.085	2.8
D_c	m/sec	6300	6360	5740
d_c	ft	12.1	7.0	436

¶ Binder compositions: PU—polyurethane, $C_{5.15}H_{9.59}O_{1.68}N_{0.14}$; PBAN (ANB-3226)—polybutadiene, acrylic acid, and acrylonitrile, $C_{6.61}H_{10.51}O_{0.55}N_{0.09}$; PVC/DOA—polyvinyl chloride and dioctyladipate, $C_{4.78}H_{8.48}O_{0.61}Cl_{0.7}$.

The computed critical diameter and detonation velocity as a function of porosity for AP-PU is plotted in Fig. 4. The porous case critical diameters in Fig. 4 are approximately 50% lower than those in Ref. 1 because the binder was allowed to burn in the current study (it was not in Ref. 1). The detonation velocities obtained with the binder burning and contributing energy are significantly greater than those without binder burning, leading to the lower d_c's. Solutions found without the binder burning (BB) duplicated prior results;** the only difference in models is that, in the current case, the void radius is subtracted from R_e. This amounts to only 5% of R_e at a porosity of 1%.

Although it is felt that the single particle model is physically unrealistic the results in Table 2 and Fig. 4 do substantiate the methods used and bring the results of Ref. 1 into perspective.

Critical Diameter of ANB-3226 Propellant

Reference 2 presents experimental results for ANB-3226 propellant. These results indicate a critical diameter for this material of $5.3^{+0.7}_{-0.3}$ ft and a critical detonation velocity of 3200 m/sec. These values are used in this study as a guide to: 1) the validity of the detonation model and the consistency of the theory; 2) the choice between binder burning (BB) or not (NBB); and 3) as a basis for determining intrinsic porosity.

The ANB-3226 nonporous solution utilizes the dual grain model shown in Fig. 1. For this model, the large AP grains will ignite at the AP Hugoniot temperature whereas the small

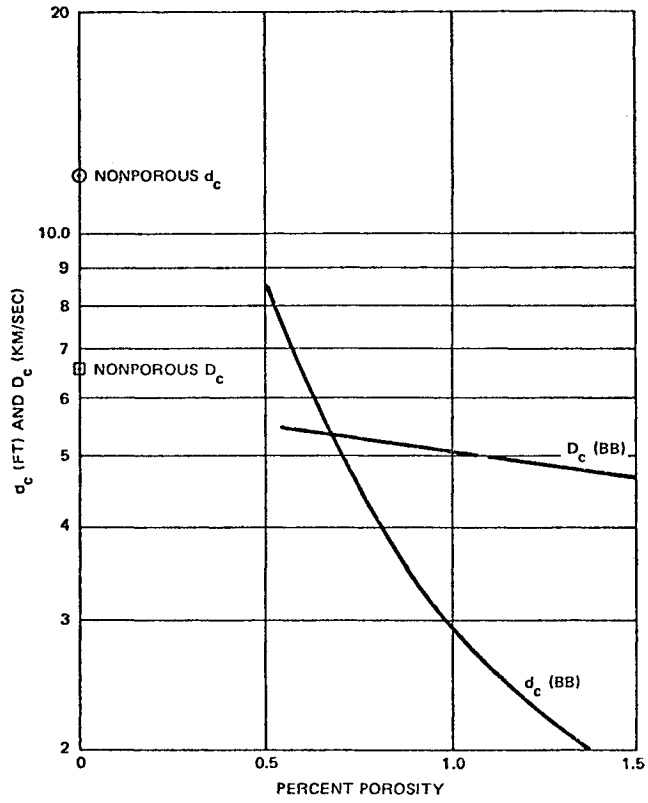

Fig. 4 Predicted critical diameter and detonation velocity of AP-PU.

** In Ref. 1 it was concluded that binder does *not* burn because the d_c's for this case were lower than when binder does burn. Because the ignition and binder burning times were reduced in the current study we find the opposite to be the case [i.e., lower d_c's *with* binder burning (see Table 2)]. On this basis the (single grain) model is physically reasonable, i.e., the oxidizer grains are sufficiently separated that burning from grain to grain without binder reaction is unlikely.

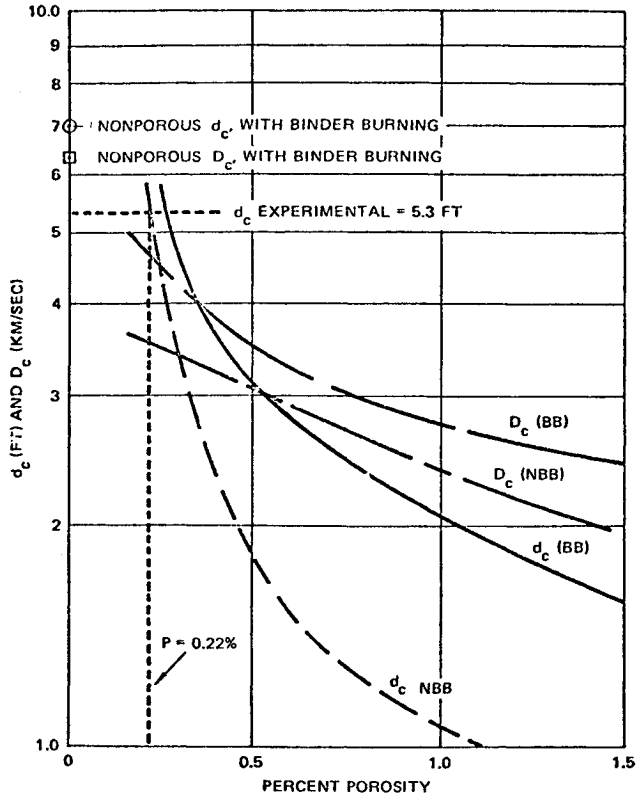

Fig. 5 Predicted critical diameter and detonation velocity of ANB-3226.

grains will cool to the equilibrated temperature with the binder and not ignite in the reaction time obtaining. Also, the large grains are large enough such that (almost) the whole particle will be at the same temperature at ignition resulting in nearly complete consumption and very little or no oxidizer burning. Therefore, following ignition, burning will proceed outward from the (large) grain surface a distance $\delta_L/2$ (see Fig. 1). The total reaction time is then given by Eq. (9).

The nonporous critical diameter solution with BB is 7.0 ft (Table 2). This low value is due to the high ideal detonation velocity[14] 6700 m/sec which causes a high Hugoniot temperature of the large grains and subsequent low ignition times. Furthermore, the binder thickness between the small AP grains is very small, resulting in rapid diffusion and binder burning.

For the case of no binder burning (NBB) the shock velocities (D_i = 4220 m/sec) and temperatures are so low that the ignition time t_i and d_c are very large. Because realistic values of d_c are possible when the binder does burn, this case was not considered.

Considering next the porous case, the dual grain porous theory was used with an oxidizer burning rate of 200 cm/sec and a $\mathscr{D}$ of 5.45×10^{-6} cm^2/sec. These are based on the same conditions as discussed for the AP-PU. The calculated critical diameters and detonation velocities with and without binder burning are presented in Fig. 5.††

†† At low values of P the d_c vs P curves are increasing rapidly and do not extrapolate to the nonporous d_c given. This implies that in this region the distance between sites ($2R_e$) and thus the burning time (t_{ob}) is large enough such that the ignition time of the small particles at the equilibrated temperature becomes significant. They are igniting because of shock heating before being consumed in the general burning. The value of P at which the effect is significant is not known. Detailed computations of t_i and t_{ob} in this region are necessary to evaluate the proper extrapolation; it may or may not be "smoothly" connected to the d_c vs P curve shown. Although the effect might lower the estimated "intrinsic porosity" the general conclusions developed in the analysis would remain unchanged (there is no effect on the D_c vs P curve). We assume the effect does not occur in the range of P of concern.

Table 3 Intrinsic porosity evaluation ANB-3226

	Binder burning (BB)		No binder burning (NBB)	
d_c ft	D_c m/sec	P %	D_c m/sec	P %
6	4550	0.24	3580	0.21
5.3[a]	4420	0.26	3530	0.22
5	4350	0.28	3500	0.23

[a] D_c experimental = 3200 m/sec (Ref. 2).

Both cases (BB and NBB) give critical diameters of the right order of magnitude. The more rapid burning rate in the NBB case generally tends to reduce the critical diameter compared to the BB case. Conversely, the lower detonation velocity in the NBB case tends to increase d_c (fewer effective voids); however, since the velocity is not substantially different from the binder case, the former effect prevails. The NBB d_c is smaller than the BB d_c as opposed to the case for AP-PU.

The BB and NBB cases are compared in Table 3 for the critical diameter range reported.[2] The D_c values for the BB case are significantly higher than the experimental value of 3200 m/sec. The NBB case however, is in reasonable agreement with experiment; at d_c = 5.3 ft,[2] the predicted D_c is only 10% greater than the experimental D_c. On this basis, it is presumed that binder burning does not take place.

As seen in Fig. 5 and Table 3, the value of porosity (most) consistent with the reported d_c and D_c is 0.22%. Since the tests with ANB-3226 were made with nominally "nonporous" propellant[2] it is hypothesized that the abovementioned figure represents the "intrinsic" porosity discussed earlier. It is notable that the value obtained falls within the bounds presumed to be reasonable. It is further speculated that this value of intrinsic porosity is reasonably constant and applicable generally to composite propellants of this type.

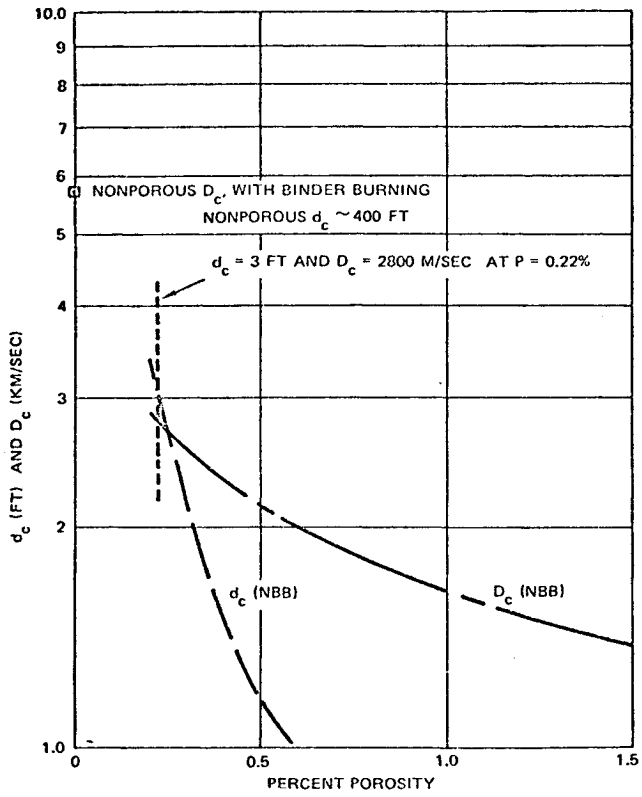

Fig. 6 Predicted critical diameter and detonation velocity of AP-PVC/DOA.

Critical Diameter of AP-PVC/DOA

The computation of the AP-PVC/DOA critical diameter was performed in the same manner as that of the ANB-3226. This propellant has a much lower ideal detonation velocity than ANB-3226 resulting in a lower AP shock temperatures and much longer ignition times. Again, the large grains will be at the AP shock temperature while the small grains will equilibrate with the binder. Considering a detonation velocity D_i of 5820 m/sec (binder burning) the temperature of the large grains is 1085°K while the small grains are at 1000°K. This results in an ignition time of 0.0014 sec for the large grains and 0.0074 sec for the small grains; the large grains will ignite first. Further, because of the small thicknesses of binder ($\delta_S = 1\mu$) the burning between grains (i.e., the binder/small oxidizer burning time) is very rapid and $t_{ob} \ll t_i$. Therefore, the small grains will not have time to self-ignite and the reaction time, and hence the critical diameter, will depend primarily on the ignition time t_i. Because of the (relatively) low detonation velocity and consequent long ignition time, the nonporous critical diameter with binder burning (BB) is found to be quite large, ~400 ft, as presented in Table 2. Therefore, the detonation of AP-PVC/DOA requires "intrinsic" porosity.

In the porous solution, B is again 200 cm/sec and $\mathscr{D}$ is now 4.85×10^{-4} cm^2/sec. For the NBB case, D_i is 4720 m/sec. The predicted critical diameter of AP-PVC/DOA is presented in Fig. 6 as a function of porosity.‡‡ The critical diameter d_c clearly decreases rapidly with porosity. Considering a value of $0.22 \pm 0.01\%$ as determined for ANB-3226 (Table 3), and without binder burning, the predicted critical diameter of AP-PVC/DOA is 3.0 ± 0.2 ft, and the predicted critical detonation velocity is 2800 ± 30 m/sec. The results are reasonable and clearly in the range of practical interest.

Conclusions

A burning model based on "hot spot" (gas-filled voids) ignition that predicts the critical diameter of composite propellants has been developed. The mathematical techniques were verified by applying the theory to a previously analyzed AP-PU propellant. The theory was then applied to an AP-PBAN propellant for which there are experimental data, ANB-3226. The results obtained support the validity of the detonation model developed; no inconsistencies arise in its application. Furthermore, it is concluded that when porosity is present in a dual grain propellant, the binder does not contribute to the detonation reaction and that the intrinsic porosity of ANB-3226 (and composite propellants in general) is ~0.2%.

The theory was then applied to an AP-PVC/DOA propellant. A critical diameter of 3 ft at a detonation velocity of 2800 m/sec was obtained.

‡‡ At the higher porosities ($P \gtrsim 1.2\%$) the critical detonation velocities approach those of the sound velocity. The solutions in this region may not be realistic.

References

[1] Salzman, P. K., Irwin, O. R., and Andersen, W. H., "Theoretical Detonation Characteristics of Solid Composite Propellants," *AIAA Journal*, Vol. 3, No. 12, Dec. 1965, pp. 2230–2238.

[2] Elwell, R. B., Irwin, O. R., and Vail, R. W., "Project Sophy—Solid Propellant Hazard Program," TR AFRPL-TR-67-211, Aug. 1967, Vol. 1, Air Force Rocket Propulsion Lab., Research and Technology Division, Edwards Air Force Base, Moffett Field, Calif.

[3] Jones, H., "A Theory of the Dependence of the Rate of Detonation of Solid Explosives on the Diameter of the Charge," *Proceedings of the Royal Society (London)*, A189, 1947, p. 415.

[4] Eyring, H., Powell, R. E., Duffy, G. H., and Parlin, R. B., "The Stability of Detonation," *Chemistry Review*, Vol. 45, 1949, p. 69.

[5] Andersen, W. H. and Chaiken, R. F., "Detonability of Solid Composite Propellants," *ARS Journal*, Vol. 31, 1961, p. 1379.

[6] Evans, M. W., "Detonation Sensitivity and Failure Diameter in Homogeneous Condensed Materials," *Journal of Chemistry and Physical Review*, Vol. 36, 1962, p. 193.

[7] Miller, R. C., "Estimating Caloric State Behavior in Condensed Phase Detonations," *ARS Progress in Astronautics and Rocketry: Detonation and Two Phase Flow*, edited by S. S. Penner and F. A. Williams, Academic Press, New York, 1962.

[8] McGurk, J. L., "Microscopic Determination of Near Solid State Changes in Aged Propellants," *AIAA Journal*, Vol. 3, No. 10, Oct. 1965, pp. 1890–1895.

[9] Sarnu, S. F., *Propellant Chemistry*, Reinhold, New York, 1966.